Universität Potsdam

Ralf Engbert, Christian Scheffczyk, Ralf Thomas Krampe,
Mikhael Rosenblum, Jürgen Kurths, Reinhold Kliegl

Tempo-induced transitions in polyrhythmic hand movements

NLD Preprints ; 41

Tempo-induced transitions in polyrhythmic hand movements

R. Engbert[(1)], C. Scheffczyk[(1)], R.T. Krampe[(2)], M. Rosenblum[(1)], J. Kurths[(1)], and R. Kliegl[(2)]
[(1)] *Institut für Theoretische Physik und Astrophysik,*
[(2)] *Institut für Psychologie,*
Universität Potsdam, Postfach 601553, D–14415 Potsdam, Germany
email: ralf@ik.uni-potsdam.de
(Physical Review E — submitted: March 10, 1997; revised: July 2, 1997;
editorially approved for publication: August 8, 1997)

We investigate the cognitive control in polyrhythmic hand movements as a model paradigm for bimanual coordination. Using a symbolic coding of the recorded time series, we demonstrate the existence of qualitative transitions induced by experimental manipulation of the tempo. A nonlinear model with delayed feedback control is proposed, which accounts for these dynamical transitions in terms of bifurcations resulting from variation of the external control parameter. Furthermore, it is shown that transitions can also be observed due to fluctuations in the timing control level. We conclude that the complexity of coordinated bimanual movements results from interactions between nonlinear control mechanisms with delayed feedback and stochastic timing components.

PACS number(s): 87.10.+e,87.45.Dr,05.45.+b

I. INTRODUCTION

The analysis of dynamical processes underlying brain functioning and behavior has evolved into a field of extensive research. In particular, the theory of complex systems [1] is a promising contribution to these problems from the viewpoint of theoretical physics. This approach is based on the notion of qualitative changes induced by variation of a control parameter of the system. As a prominent example, the Haken–Kelso–Bunz model [2] emphasizes the importance of qualitative transitions for the understanding of the dynamics in the control of motor behavior.

Timing of bimanual movements is an ideal experimental framework for the study of cognitive motor control. The analysis of bimanual polyrhythmic movement tasks may be looked upon as a case study for the more general problem of bimanual coordination [3]. Numerous studies have shown that bimanual coordination is subject to strong performance constraints [4]. Experimental variation of external parameters, like manipulating the required speed of performance or the difficulty of the movement pattern, permits the systematic study of how the human movement control system adapts to these external and its own internal constraints. The use of performance tempo as an external control parameter in the experiment under consideration [5] yields the new finding of transitions between qualitatively different dynamical regimes.

A crucial problem for the analysis of complex natural systems is the comparison of theoretical models with experimental data. Different from most experiments in physics, key observables in living systems are more restrictively prescribed by the measurement procedure and their functional state can be controlled to a much lower extent. By using symbolic dynamics [6] we demonstrate that, nevertheless, the comparison of theory and experiment can be achieved even at the level of individual subjects based on short and noisy time series.

The analysis of physiological and psychological systems using nonlinear methods of data analysis [11,12] is promising to gain new insights into the complex interactions between subsystems and the resulting dynamical behavior. The more traditional approach to the analysis of human movement timing has employed linear models of covariance structures between the produced time intervals [5,13,14]. Related methods rest on strong statistical assumptions which are often violated and also require data aggregation to a degree that precludes investigation of interesting qualitative phenomena on the basis of individual performance which is an important advantage of our methods of time series analysis.

A considerable number of studies has focused on the variability in the control of movements. In the framework of timer–motor or two–level models (for review cf. [14]), it has been shown that the observed variability can be exploited to analyze the organization of control structures in the brain. At the same time nonlinear dynamical models have explained the occurrence of phase transitions in behavior [1], at least at a qualitative level.

The typical approach to the study of the stability of rhythmic performance is the analysis of dynamical transitions which occur when high-order polyrhythms, e.g. 3:8, fall apart in response to increasing external tempo constraints during performance [7–10]. Related experiments were designed for the observation of transitions between polyrhythms of different order. In contrast to this we demonstrate here the existence of qualitative changes in the stable production of the same polyrhythm when it is performed at different tempi. The concepts of nonlinear dynamics and timer–motor models are combined. We propose a stochastic timer for the control of cycle durations in combination with deterministic feedback control.

In Sec. II we present the design of our experiment.

The analysis of the corresponding data, in particular the oberservation of qualitative transitions, is given in Sec. III. Our nonlinear model, which is introduced in Sec. IV, reproduces these dynamical transitions. Furthermore, it permits the inclusion of realistic random fluctuations in timing.

II. EXPERIMENTAL SET-UP

The 3:4 polyrhythmic task (Fig. 1) was performed on an electronic piano with a weighted keyboard mechanic hooked to a computer which monitored the experiment and recorded time-stamped data with a resolution of 1 ms. Fourteen different metronome tempi ranging from 600 ms per cycle to 8200 ms per cycle were presented in a randomized order. Error trials or trials with more than 10% deviation from the prescribed timing pattern were discarded. The data reported in this paper came from well-trained amateur pianists (for details cf. [5]).

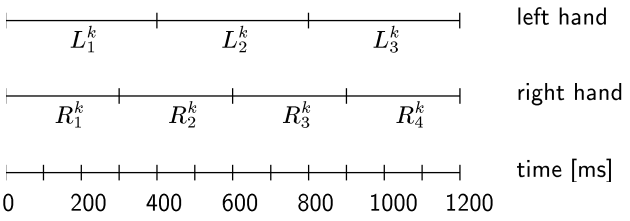

FIG. 1. Schematic illustration of the 3:4 polyrhythmic task used in the study by Krampe et al. (1996); here for a cycle duration of 1200 ms. "R" and "L" in the top panels denote the intervals produced by right and left index fingers, respectively. Each cycle starts with simultaneous strokes of the two hands. Three isochronous intervals, i.e. equidistant strokes in time, in the left hand are performed against four isochronous intervals in the right hand within each cycle. The position of intervals within a certain cycle k is indicated by sub-indices.

In each trial, subjects listened to the exact rhythm generated by the computer as long as they wanted, and then played along (synchronized) with the beat for four cycles after which the computer beat stopped. Participants had to continue for another 12 cycles during which the time series were recorded. Hence, a single time series consists of 12 bars or cycles. The recorded data are the intervals between successive keystrokes produced by both hands,

$$L_1^1,\ L_2^1,\ L_3^1,\ L_1^2,\ L_2^2,\ \ldots\ L_2^{12},\ L_3^{12}\ , \tag{1}$$

$$R_1^1,\ R_2^1,\ R_3^1,\ R_4^1,\ R_1^2,\ \ldots\ R_3^{12},\ R_4^{12}\ . \tag{2}$$

III. DATA ANALYSIS

Our method to analyze these data consists of two main parts: First, we transform the recorded time series into a sequence of symbols. This can be used as a powerful visualization technique. If a transformation to symbolic strings is applied to a time series, a considerable amount of information is discarded, but nevertheless characteristic properties of the underlying dynamics can be captured by the symbol sequence [15]. In a second step, we apply the concept of measures of complexity [16] to the symbol sequences in order to get a quantitative evaluation of the distribution of symbols [17].

A. Symbolic dynamics as a visualization technique

A straightforward coding of the time series would be to assign a '0' to those intervals which are too short and a '1' for those which are too long. This symbolic transformation, however, is sensitive to fluctuations and trends of the cycle duration, which are considerable within a single trial. We compare the produced intervals with the realized tempo for each cycle. Let us denote the realized duration of the k^{th} cycle ($k = 1, 2, 3, ..., 12$) by t^k, defined as the sum of the subintervals of the corresponding hand (t_L^k and t_R^k respectively). The relative deviations are defined as

$$l_i^k = \frac{3L_i^k - t_L^k}{t_L^k}\ , \quad r_j^k = \frac{4R_j^k - t_R^k}{t_R^k}\ , \tag{3}$$

where $i = 1, 2, 3$ and $j = 1, 2, 3, 4$. These are the deviations from the prescribed rhythm regardless of the accuracy in overall tempo. The motivation for this transformation is as follows: If a subject holds the prescribed tempo within acceptable tolerance, then the relative deviations (3) quantify the precision of the rhythmic structure of the performance. However, it must be kept in mind that this is not an absolute measure of performance accuracy.

We further reduce the amount of data by a transformation into symbol sequences. This simplifies the investigation to the analysis of the symbol patterns. Our strategy is to use such a coarse-graining of the data in order to explore important structures of the underlying dynamics.

In the following we use only two symbols ('0' and '1'). Let us consider the transformed left hand time series (3) as an example. To each value of the relative deviation l_i^k ($i = 1, 2, 3;\ k = 1, 2, ..., 12$) we assign a symbol s_n in the following way:

$$s_n = \begin{cases} 0, & \text{if } l_i^k < 0 \\ 1, & \text{otherwise} \end{cases}\ , \tag{4}$$

where $n = 3(k-1) + i = 1, 2, 3, ..., 36$. This coding scheme is called static, since we use a fixed threshold in the conditional part. Such a symbolic description can be progressively refined by introducing more symbols. The appropriate number of symbols is practically limited by the length of the time series from which the symbol sequence is derived, because the statistical confidence level

of the occurrence of the symbols drops down. Furthermore, plots with many different symbols (e.g. more than 5) are much more difficult to interpret visually.

The symbol sequences obtained by the coding of all trials produced by subject A, a well-trained amateur pianist, are shown in Fig. 2(a). Any type of regularity in the symbol sequences indicates a systematic deviation from the prescribed rhythm. On the other hand, near-perfect performance would yield a completely random pattern, since the relative deviations (3) would be randomly negative or positive with a small absolute value.

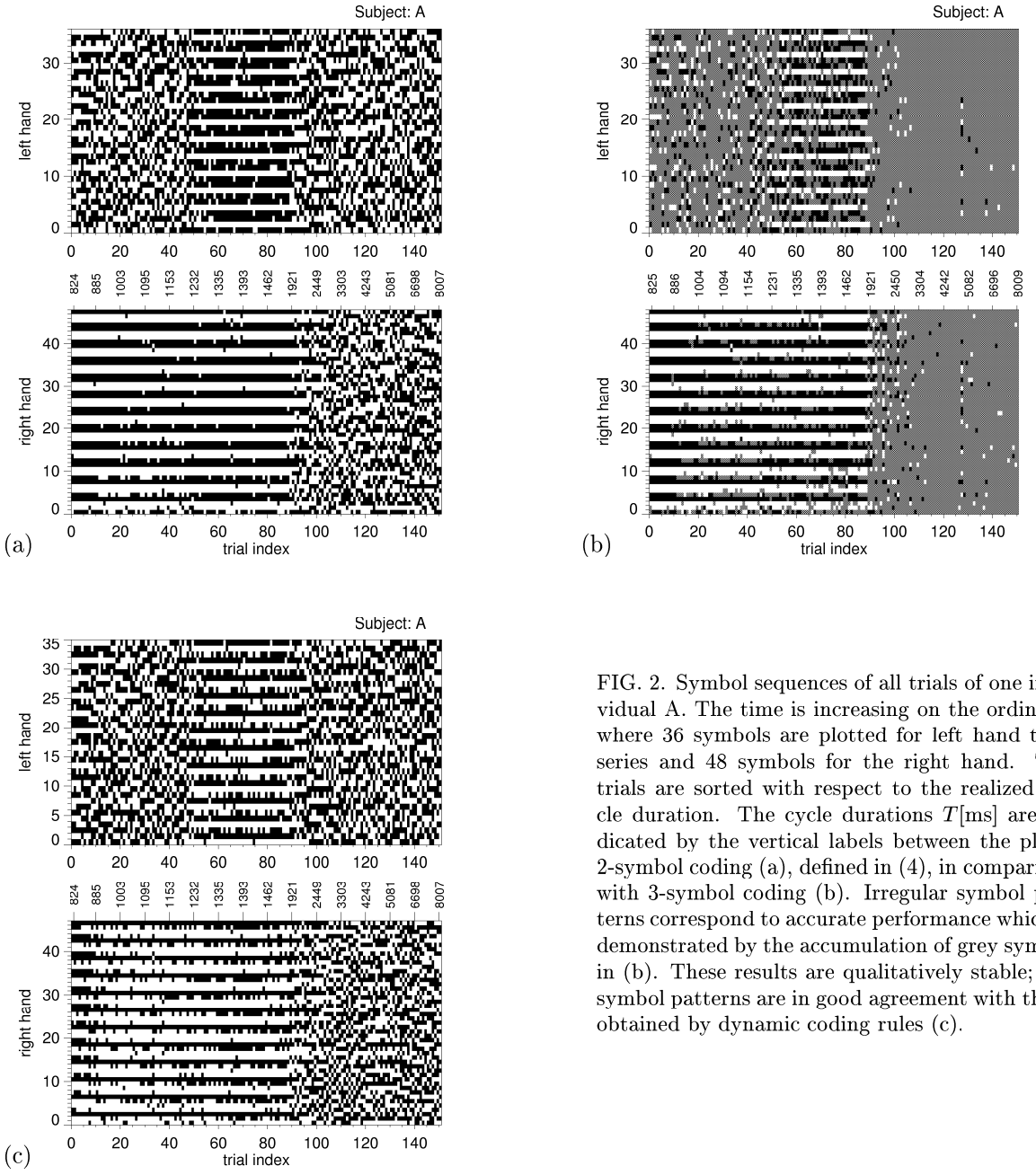

FIG. 2. Symbol sequences of all trials of one individual A. The time is increasing on the ordinate, where 36 symbols are plotted for left hand time series and 48 symbols for the right hand. The trials are sorted with respect to the realized cycle duration. The cycle durations T[ms] are indicated by the vertical labels between the plots. 2-symbol coding (a), defined in (4), in comparison with 3-symbol coding (b). Irregular symbol patterns correspond to accurate performance which is demonstrated by the accumulation of grey symbol in (b). These results are qualitatively stable; the symbol patterns are in good agreement with those obtained by dynamic coding rules (c).

A completely random pattern would also emerge in the case of large (but random) fluctuations around the prescribed timing pattern. Therefore, we introduce a second (more refined) symbolic coding to our data in order to check our interpretation that the subject performs the rhythm more exactly in the irregular regions of the symbol plot (Fig. 2(a)). This can be done by adding a third symbol to the transformation (4) for a rather exact performance. It is related to the case of a deviation of less than 5% from the realized interval duration, i.e. s_n is defined as in (4), but additionally $s_n = 2$, if $|l_i^k|$ or $|r_j^k| < 5\%$. The corresponding symbol patterns (Fig. 2(b)) demonstrate that the transition from nearly periodic symbol sequences to irregular ones in the right hand of subject A occurs simultaneously with a significant increase in the mean accuracy which is indicated by the increase in the number of grey symbols ($s_n = 2$) for increasing cycle durations.

We observe two order–disorder transitions in Fig. 2(a). One transition occurs in both hands at a cycle duration of about 1.9 s. When the tempo is increased, a second transition to irregular symbol sequences happens in the left hand at about 1.2 s. This indicates that the left hand performs more accurately for a faster tempo.

The technique of symbolic codings is a visualization tool which can extract structures from rather short (12 cycles) and noisy time series. To obtain clear results one has to find a suitable class of coding rules. The qualitative structure of the symbol patterns, however, turns out to be rather stable. This can be demonstrated by a dynamic coding scheme, which represents a different type of symbolic transformation [16]. In this coding we map an interval R_j^k, L_i^k of the original time series (1,2) to a '0', if the actual value is smaller than its preceding value, and to a '1', if it is larger. In the corresponding symbol plot (Fig. 2(c)) we observe transitions at the same positions. In contrast to Figs. 2(a,b) this dynamic symbolic coding is more sensitive to noise, since its threshold in the coding rule is not fixed at a certain value.

B. Statistics of symbols and measures of complexity

Now we outline the main ideas how the symbol sequences can be used for a quantitative study of the dynamics of polyrhythms. Due to the fact that the basic rhythmic structure is a cycle, it is appropriate to subdivide the time series into substrings or 'words' of 3 (left hand) or 4 (right hand) symbols and to study the occurrence of these words. To give an example, subject A (Fig. 2(a)) uses almost exclusively the right hand word '0110' for bar durations $T < 2$ s, i.e. the first and last interval of each bar is too short, whereas the two other intervals are too long. From the definition of the relative deviations (3) it is clear that $\sum_{i=1}^{3} l_i^k = \sum_{j=1}^{4} r_j^k = 0 \quad (k = 1, 2, ..., 12)$, implying that words consisting entirely of '0's or '1's are impossible. Therefore, we retain $N_w^L = 2^3 - 2 = 6$ possible words for the left and $N_w^R = 2^4 - 2 = 14$ words for the right hand.

The relative frequency $p_i = N_i/N_w$ of word i is calculated using all cycles generated during several trials at a certain tempo. The corresponding relative frequency distribution is denoted by p. For the data in Fig. 2(a) the fact that the subject uses almost exclusively the word '0110' in the right hand leads to a strongly peaked probability distribution.

To distinguish different kinds of probability distributions, we calculate the well-known Shannon entropy of the distribution p,

$$S(p) = -c \sum_{i=1}^{N_w} p_i \ln p_i \ , \tag{5}$$

here normalized with respect to the number of all words N_w using $c = 1/\ln N_w$. The qualitative changes in the symbol pattern are correctly described by the Shannon entropy (Fig. 3(a,b)). In particular, the two transitions in Fig. 2(a) (left hand, above) are reflected in two sharp transitions in the Shannon entropy. Applying algorithmic complexity (cf. [16]) to the symbol sequences leads to comparable results.

It is important to note that linear measures for the fluctuations or accuracy, e.g. covariances, show a much smoother transition which cannot be identified reliably at the level of individuals. The significance of our results has been tested by analyzing computer-generated random patterns of the same data length. For each experimentally observed time series we simulate a Monte-Carlo time series using the same variances of intervals as in the original data (Fig. 3(a,b)). The corresponding Shannon entropy (dashed line) is significantly higher than the entropy of the original data in those regions where regular symbol sequences occur.

The dynamical transitions can also be visualized by an analysis of the relative phases (e.g. [7]). If we define the phase of the left (slow) hand as linear increasing from 0 to 2π between two successive strokes, then we can determine the relative phase of the three strokes of the right hand with respect to the phase of the left hand. If the performance is perfect, then we can read off these relative phases directly from the task sketch in Fig. 1. We obtain a relative phase of $\frac{3}{2}\pi$ for the first stroke of the right hand, π for the second, and $\frac{1}{2}\pi$ for the third stroke. In the plot of relative phases (Fig. 3(c)) we observe that these predictions are fulfilled by subject A in the range of slow tempi (trial index greater than 100). For faster performance considerable deviations occur. In particular, the relative phase of the third stroke of the right hand is increasing from $\frac{1}{2}\pi$ to π. For trials 60 to 85 we notice a plateau region of the relative phase. Therefore, the analysis of relative phases also proves the existence of dynamical transitions. A comparison with Fig. 3(a,b) shows, however, that the plots of the Shannon entropy can extract three different dynamical regimes more clearly.

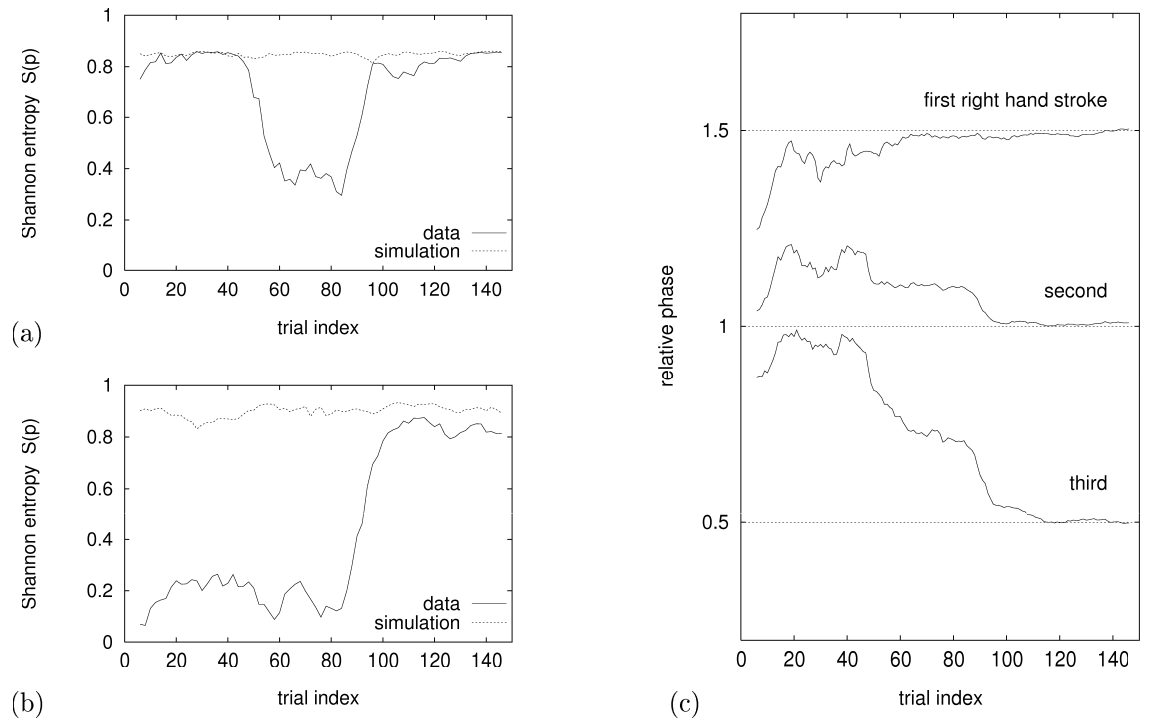

FIG. 3. Shannon entropy (5) of the distribution of words obtained from the data of subject A (left hand (a), right hand (b)). A low value of the $S(p)$ corresponds to highly regular symbol sequences. The dashed line shows the Shannon entropy for simulated data (surrogates) using the variances as in the experimental time series. (c) A plot of the relative phases (in units of π) also indicates the dynamical transitions.

C. More examples

The data produced by two other subjects are visualized in Fig. 4 using the 2-symbol coding (4) and the corresponding Shannon entropies. As for subject A, the variation of tempo or cycle duration T, our external control parameter, enables us to observe qualitative transitions.

An example of a rather sharp transition occurring in the right hand is the one at cycle duration $T \approx 2$ s in Fig. 4(a), approximately at trial number 90. In Fig. 4(c), a transition can be seen in the left hand at $T \approx 1.5$ s (trial 60). Transitions can occur in the left or right hand, or even in both hands at the same tempo (subject A, Fig. 2(a)). Preliminary investigations on a larger study indicate that there is no straightforward relation to handedness. All subjects tested were right-handed. This demonstrates a complex dynamical interaction of the hands.

The fact that the transitions do not always occur in the fast range of tempi is very important. As an example, a regular symbol pattern in an intermediate range of cycle durations (between 1.5 s and 3.5 s) is observed in the data set produced by subject C (Fig. 4(c)). It implies that the transitions are a consequence of nonlinearity in the human movement control system, rather than a result of increasing biomechanical constraints at fast tempi ($T < 2$ s). Furthermore, the Shannon entropy for the left hand of subject B (Fig. 4(b)) and for the right hand of subject C (Fig. 4(d)) indicate that the corresponding symbol patterns are not completely random. Instead these patterns show subtle periodic structures which we also see by visual inspection. In these cases the dynamics may be close to a qualitative transition.

We now use the results of our data analysis to develop a dynamical model which exhibits the same type of transitions as found in the experiments. We stress the importance of the finding of qualitative changes and their description by appropriate techniques as an ideal starting point for deriving conceptual models.

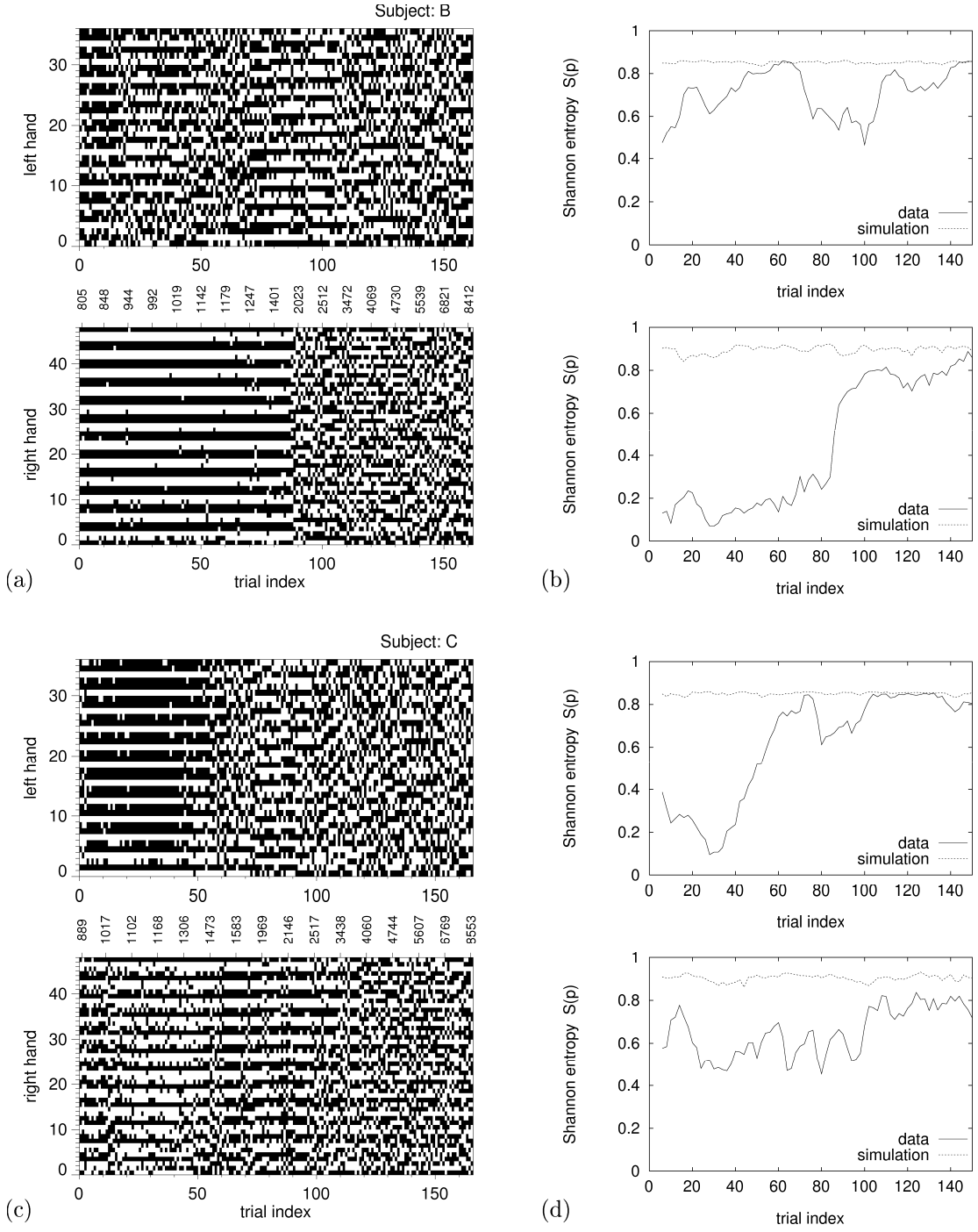

FIG. 4. Symbol sequences of all trials and corresponding Shannon entropies for two other individuals obtained by the 2-symbol coding. The data of subject B (a,b) show a sharp transition in the right hand, whereas the data of subject C (c,d) are an example for a qualitative transition in the left hand.

IV. MODELING

A. Nonlinear error correction

A considerable amount of theoretical work on the production of rhythmic movements focuses on stochastic models without error correction. In this framework, the dynamical structures, e.g. the patterns of covariances between intervals, are explained by different stochastic variables operating in a hierarchical organization (cf. [14] for a review). Qualitative transitions cannot arise from the dynamics of these models.

Different from this purely stochastic approach, we aim at a dynamical explanation of the observed qualitative transitions. Therefore, we have to include a nontrivial deterministic component of the dynamics, comparable to the well–known Haken–Kelso–Bunz model [2]. We start with an equation for error correction of single–handed movements,

$$x_{i+1} = \delta_{i+1} + k \tanh[\alpha(x_i - \delta_i)] \; . \tag{6}$$

In this model an interval x_{i+1} is produced by a stochastic variable (timekeeper) δ_{i+1} and an error correction term. The error correction operates with respect to the deviation $x_i - \delta_i$ of the last interval from the last timekeeper value. For small deviation we assume a linear error correction. For larger deviations there is a saturation effect. This is a common type of nonlinearity in biological systems which could be motivated in our case by a constant rate of information processing in the human movement control system. With the two parameters α and k we can adjust the slope and the asymptotic value of the correction function separately.

In the deterministic case, i.e. $\mathrm{var}(\delta) \to 0$ or $\delta_i \equiv \delta_0$ for all i, a linear transformation of variables, $z_i = \alpha(x_i - \delta_0)$, leads to the system

$$z_{i+1} = c \tanh(z_i) \; , \tag{7}$$

where $c = k\alpha$ is the control parameter. The qualitative behavior of this equation can be described by a bifurcation diagram [18]. For $|c| < 1$ model (6) generates the same qualitative behavior as a model with linear error correction (Fig. 5). The asymptotic solution is $z = 0$, a fixed point. If $|c| > 1$, then this solution becomes unstable. Different from linear models, equation (6) creates two additional fixed points. For $c = 1$ there is a pitchfork bifurcation with a positiv and a negativ branch. The asymptotic value of z depends on the initial conditions. For $c = -1$ there is a period–doubling bifurcation which creates an oscillatory solution. This period–doubling bifurcation of period 2 can explain the occurrence of periodic symbol patterns in the experiments. Therefore, we use basically two equations of type (7) for our modeling of bimanual movements.

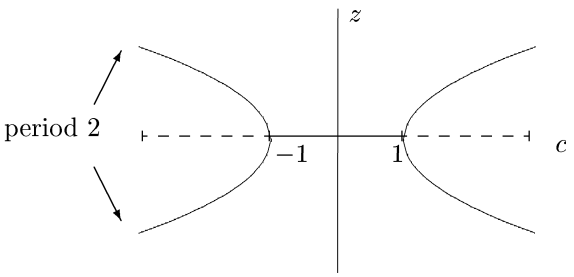

FIG. 5. Bifurcation diagram of the nonlinear error correction model (6). A pitchfork bifurcation occurs at $c = +1$. The period–doubling bifurcation ($c = -1$) creates oscillating solutions for $c < -1$ which are the basis for reproducing the periodic symbol sequences obtained from the experiments.

B. A nonlinear model for the production of polyrhythms

Our model is formulated for the production of polyrhythmic movements of arbitrary order, i.e. N^r strokes per cycle with the right hand versus N^l strokes with the left hand. For the experiments discussed here, we fix $N^r = 4$ and $N^l = 3$. The tempo (or cycle duration) is denoted by δ. Because of considerable fluctuations δ is used as a random variable, where δ_c is its realization in cycle c. The stochastic properties of δ will be treated below. The required interval durations for the hands are $\delta_c^r = \delta_c / N^r$ and $\delta_c^l = \delta_c / N^l$.

The deterministic control loop of our model consists of two coupled maps which generate the interval durations of the subsequent strokes for the right x_j^r and the left x_i^l hand respectively,

$$\begin{aligned} x_{j+1}^r &= \delta_c^r \overbrace{-\Delta_j^r k_1^r \tanh[\alpha_1^r (x_{j-d}^r - \delta_{c-1}^r)]}^{\text{(I)}} \\ &\quad \underbrace{- \Theta_j^r k_2^r \tanh[\alpha_2^r (\hat{\delta}_c^r - \hat{\delta}_c^l)]}_{\text{(II)}} \; , \\ x_{i+1}^l &= \delta_c^l \overbrace{-\Delta_i^l k_1^l \tanh[\alpha_1^l (x_{i-d}^l - \delta_{c-1}^l)]}^{\text{(I)}} \\ &\quad \underbrace{- \Theta_i^l k_2^l \tanh[\alpha_2^l (\hat{\delta}_c^l - \hat{\delta}_c^r)]}_{\text{(II)}} \; , \end{aligned} \tag{8}$$

where $c = \lfloor (j-1)/N^r \rfloor + 1 = \lfloor (i-1)/N^l \rfloor + 1$ is the cycle index and $\lfloor . \rfloor$ denotes the integer part of the included expression. To each subinterval $x_i^{r,l}$ we assign the value of the stochastic duration $\delta_c^{r,l}$ according to (20), with respect to the actual tempo δ_c of the cycle. This value is then corrected by two feedback mechanisms: The first correction term (I) is active within the cycle and the coupling term (II) is only active at the end of each cycle.

This is fulfilled by defining

$$\Delta_i^{r,l} = \begin{cases} 1, & \text{if } (i+1) \bmod N^{r,l} \neq 0 \\ 0, & \text{otherwise} \end{cases} , \tag{9}$$

$$\Theta_i^{r,l} = \begin{cases} 1, & \text{if } (i+1) \bmod N^{r,l} = 0 \\ 0, & \text{otherwise} \end{cases} . \tag{10}$$

Now we discuss the different terms in the model equations (8) in detail:

(I) The first correction operates within a cycle, i.e. dynamical correction is performed separately for each hand. Previous investigations [19] have shown that this correction has to incorporate two essential properties in order to reproduce the experimentally observed symbol patterns.

  (a) The first property is a *nonlinear correction function*. As in (6) we have chosen a tanh-function here, a piecewise linear function or any sigmoid function would also be a possible choice. This nonlinearity enables the model to reproduce the bifurcations underlying the experimentally observed periodic symbol sequences.

  (b) The second important feature is that the correction operates with a *time delay* d. In some cases $d = 0$ yields to the observed symbol patterns. On the other hand, a delay time $d \geq 2$ would lead to symbol patterns with a period longer than a cycle which is never found in the experimental data [19]. Therefore, to explain almost all of the observed periodic symbol patterns, we fix $d = 1$.

(II) The coupling mechanism aims at the synchronization of the movements of the hands and is performed at the end of each cycle with a strength given by parameters k_2^r and k_2^l. The coupling of the hands is done on the basis of a prediction of the *estimated cycle durations* $\hat{\delta}_c^r$ and $\hat{\delta}_c^l$ of the cycle c. Here we use

$$\hat{\delta}_c^r = N^r x_{i-d}^r , \quad \hat{\delta}_c^l = N^l x_{i-d}^l . \tag{11}$$

  The explicit form of these estimations determines the type of symbol pattern that are produced by the model. The correction function is the tanh-function as in (I).

Some additional remarks on these assumptions are necessary: First, if the within-hand correction is the only type of feedback control, then a stochastic detuning ϵ would lead to a desynchronization of the hands. As a consequence, the simultaneous stroke at the end of each cycle would fail. In contrast to this, our experiments show that subjects were able to perform the simultaneous (last) stroke of the cycle. This is the motivation for the coupling mechanism (II).

Second, to understand the form of the estimated cycle duration, we compare the within-hand correction (I) with the coupling mechanism (II). For the within-hand correction in cycle c the value of the tempo $\delta_c^{r,l}$ is assumed to be unaccessible for the control system due to delay and fluctuations. For the coupling mechanism (II) the control system has to compare the instantaneous cycle durations δ_c^r and δ_c^l. Since their realized values are unaccessible in cycle c, we assume that those intervals which would be the basis for the within-hand correction, x_{i-d}^r and x_{i-d}^l, are also used for the coupling. Therefore, the form of the estimated cycle durations (11) is consistent with the form of the within-hand correction. Since the choice of the estimates determines the periodic symbol patterns, which can be produced by numerical simulations of the model, additional constraints arise from symbol patterns observed in the experimental data (Figs. 2(a) and 4(a,c)).

C. Analysis of the model

To demonstrate that our model can explain the structure of the symbol patterns derived from the experimental data, we now present some analytical results on the dynamics for $d = 1$. This is done in the deterministic case and for strongly nonlinear control, i.e. $\alpha \to \infty$, where $\tanh(\alpha z) \to \mathrm{sgn}(z)$. We fix $k_1^{r,l} = -1$ and $|k_2^{r,l}| = 1$. Furthermore, we assume that the dynamics is stationary and the maximal period length of the symbol sequences is a cycle, i.e. $z_j^r = x_j^r - \delta_0^r = z_{j+4n}^r$ and $z_i^l = x_i^l - \delta_0^l = z_{i+3n}^l$ for all $n = 0, 1, 2, \ldots$. Under these assumptions the model gives seven equations for the relationship of subintervals,

$$z_1^r = -\mathrm{sgn}(z_3^r) , \tag{12}$$
$$z_2^r = -\mathrm{sgn}(z_4^r) , \tag{13}$$
$$z_3^r = -\mathrm{sgn}(z_1^r) , \tag{14}$$
$$z_4^r = k_2^r \,\mathrm{sgn}(4z_2^r - 3z_1^l) , \tag{15}$$

for the right hand and

$$z_1^l = -\mathrm{sgn}(z_2^l) , \tag{16}$$
$$z_2^l = -\mathrm{sgn}(z_3^l) , \tag{17}$$
$$z_3^l = k_2^l \,\mathrm{sgn}(3z_1^l - 4z_2^r) , \tag{18}$$

for the left hand. These equations lead to four different symbol sequences in the right hand ('0011','0110','1001','1100') and two for the left hand ('010','101'). Which of the these patterns are combined is determined by the coupling. If $k_2^r = k_2^l$, then we get $z_1^r = -z_1^l$, and if $k_2^r = -k_2^l$, then we will observe symbol sequences with $z_1^r = z_1^l$. These symbolic structures are in correspondence with the experimental data. In the symbol patterns of subject A (Fig. 2(a)) we observe the periodic symbol sequences '0110' produced by the right hand for trials 1–50 and in combination with '010' produced by the left hand for trials 50–90. For subject B we also observe the pattern '0110' in the right hand for

the fast range of tempi. Additional symbol patterns, like '100' in the left hand of subject C for trials 1–50, can also be explained dynamically by the model. This can be demonstrated by numerical simulations.

An important feature of the symbol patterns is their stability, which is found in the experimental data. This has to be investigated by simulations of the model below. Now we address the stochastic properties of our model.

D. Stochastic fluctuations in timing

A realistic model of human movement timing has to include the random fluctuations observed in related experiments. We now specify the stochastic properties of the tempo variable δ. A second source of randomness is the motor system, which is discussed below.

The tempo variable δ is treated as an uncorrelated random process. For the study of qualitatively different dynamical regimes, it is important that the variance $\mathrm{var}(\delta)$ of δ is a monotonously increasing function of the mean value $<\delta>$. This fact is in good agreement with the hypothesis that the interval duration is produced by some elementary counting mechanism. The explicit form in the production rhythms, however, depends on the experimental design.

For numerical simulations of our model we estimate the relation between the mean value $<\delta>$ and the variance $\mathrm{var}(\delta)$ from the experiments. Under the assumption that the noise produced by the motor system is small compared to the fluctuations in the timing control, the bar duration t^c of cycle c can be used as an approximation to δ_c. For simplicity we assume a polynomial relation of second order [14],

$$\mathrm{var}(\delta) = a < \delta > + b < \delta >^2 , \tag{19}$$

which includes the two parameters a and b (Fig. 6). For the simulations we use gamma–distributed random variables with the required relation between mean and variance.

At this point the question arises, how the value of the stochastic variable δ_c is related to the values of δ_c^r and δ_c^l. Let us assume that there is stochastic variation in the tempo for the right and the left hand. We introduce, therefore, a detuning parameter ϵ with

$$\delta_c^{r,l} = \frac{\delta_c}{N^{r,l}}(1 + \epsilon\,\xi) , \tag{20}$$

where ξ is a uniform random deviate between -1 and 1. Analyzing the symbol patterns obtained by numerical simulations of our model yields an upper limit for the detuning parameter: $\epsilon \leq 10^{-2}$. The question whether δ_c^r and δ_c^l arise from two different, but certainly coupled timing processes is outside the scope of this work. We now discuss the inclusion of the random fluctuations which originate from the motor system.

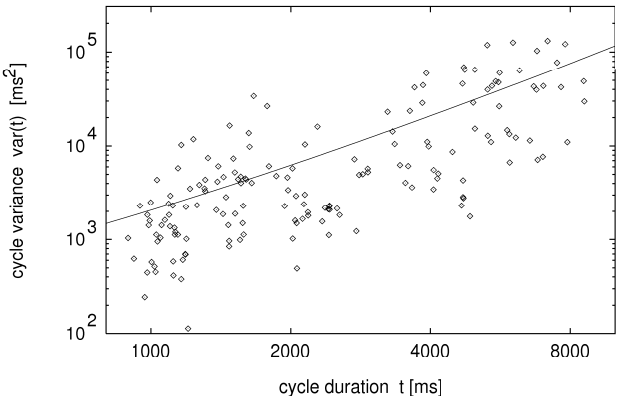

FIG. 6. Relation between cycle variance $\mathrm{var}(t)$ and mean cycle duration $< t >$ for subject C. As a rough approximation we obtain a polynomial of second order (19) with $a = 1.003$ and $b = 1.06 \cdot 10^{-3}$. Note that the time series consists of only 12 values, which contributes to the scattering of data points around the regression line.

The variables $x_i^{r,l}$ represent the control level. We implement our dynamical timing model into the framework of the so-called two-level timing [14]. The commands for the hand movements produced by the control level are executed by the motor level with some stochastic motor response. The stroke i of the right hand is performed with motor response m_i^r (Fig. 7). Therefore, the intervals $x_i^{r,l}$ observed are bounded by two motor reponses, i.e.

$$y_j^r = x_j^r + m_j^r - m_{j-1}^r , \tag{21}$$

$$y_i^l = x_i^l + m_i^l - m_{i-1}^l . \tag{22}$$

As a first approximation the motor responses $m_i^{r,l}$ are assumed to be uncorrelated and gamma–distributed random numbers which are statistically independent from the control level $x_i^{r,l}$. If the process on the control level, $x_i^{r,l}$, is also statistically independent, the two–level timing yields simple prediction on the covariances. The variance of the recorded intervals is a sum of terms arising from the two sources of variability,

$$\mathrm{var}(y_i) = \mathrm{var}(x_i) + 2\mathrm{var}(m_i) . \tag{23}$$

Since each recorded interval $y_i^{r,l}$ is affected by two motor repsonses, we observe a negative autocovariance function for lag equal one,

$$\begin{aligned} \mathrm{cov}(y_i, y_{i+1}) &= \mathrm{cov}(x_i, x_{i+1}) \\ &+\mathrm{cov}(m_i - m_{i-1}, m_{i+1} - m_i) = -\mathrm{var}(m_i) . \end{aligned} \tag{24}$$

We can use these two equations for estimating the variances of the control level and the motor system separately,

$$\mathrm{var}(m_i) = -\mathrm{cov}(y_i, y_{i+1}) , \tag{25}$$

$$\mathrm{var}(x_i) = \mathrm{var}(y_i) + 2\mathrm{cov}(y_i, y_{i+1}) . \tag{26}$$

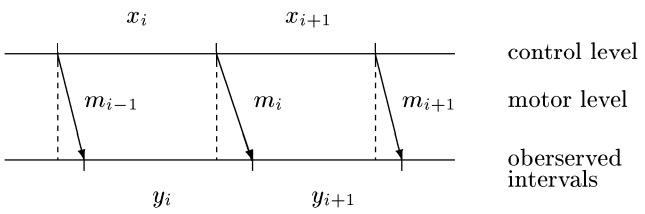

FIG. 7. Schematic illustration of two–level timing. The motor delays are uncorrelated. Due to the measurement procedure, the successive intervals are negatively correlated.

For simple tasks like unimanual tapping, where the strong assumptions of statistical independence is a valid approximation, two–level timing predicts that the timer variance (26) is increasing with the cycle duration, whereas the motor variance (25) should remain constant. This prediction has been confirmed in many cases (cf. [14] for a review), even for the more complicated case of synchronization of finger movements with a metronome. Therefore, two–level timing does not exclude error correction which is an essential property of our dynamical model.

Furthermore, there is neurophysiological evidence for the concept of two–level timing. A study of the effects of neurologic damage to the cerebellum [20] has demonstrated a dissociation effect between estimates of timekeeper interval variance and response delay variance.

E. Numerical Simulations

Now we present two examples of numerical simulations of the model. Our model is a stochastic nonlinear model. As a consequence, order–disorder transitions in the symbol patterns can be due to increase of fluctuations as well as bifurcations of the underlying deterministic control system. Generally, realistic simulations will involve both types of transitions.

The strengths of the correction mechanism are given by the value of the parameters $k_{1,2}^{r,l}$ (8). Since these parameters determine the saturation or maximal correction, it is reasonable to assume a linear dependence of the parameters on the cycle duration as a first approximation.

In the first simulation (Fig. 8(a)) we use only one control parameter ($k_1^r = -45, ..., -1$), which leads to a clear transition in the right hand. Because of the linear variation of the parameter the bifurcation point is at trial 85. The control parameter of the right hand correction is near the bifurcation point, $k_1^l \alpha_1^l = 0.7$. The coupling of the two hands induces subtle structures in the symbol pattern of the left hand, which is confirmed by the plot of the Shannon entropy (Fig. 8(b)). The other parameters are $k_1^l = -7$, $k_2^r = -10$, $k_2^l = 10$, $\alpha_1^r = 0.05$, $\alpha_1^l = 0.1$, $\alpha_2^r = 0.3$, $\alpha_2^l = 0.05$, $a = 1$, $b = 10^{-3}$, $\epsilon = 3 \cdot 10^{-3}$, $\mathrm{var}(m) = 50$, initial values: $x_0^{r,l} < 0$, $x_{-1}^{r,l} > 0$. The simulation in Fig. 8 is qualitatively in agreement with the experimental data in Fig. 4(a) (subject B).

Using a linear variation of several parameters, we can reproduce more complicated transitions. The symbol pattern of subject A (Fig. 2(a)) is an example with two transitions between regular and irregular symbol sequences in the left hand, where a regular region of symbol sequences extends approximately from a cycle duration of 1.2 s to 3 s. The parameters for a simulation with comparable qualitative features (Fig. 9) are $k_1^r = -35, ..., -30$, $k_1^l = -10, ..., -25$, $k_2^r = -8, ..., -15$, $k_2^l = 1, ..., 25$, $\alpha_1^r = \alpha_1^l = 0.06$, $\alpha_2^r = 0.3$, $\alpha_2^l = 0.08$, $a = 1$, $b = 10^{-3}$, $\epsilon = 10^{-3}, ..., 10^{-2}$, initial values: $x_0^{r,l} < 0$, $x_{-1}^{r,l} > 0$).

These two examples demonstrate that the proposed model is able to reproduce qualitative characteristics of the dynamical transitions. It is a challenge for future work to compare numerical simulations with the experimental data in order to extract the control parameters underlying the performance of individuals. Using this approach, the complexity of the dynamics of hand movements could be captured in the variation of the control parameters of the dynamical model (8). To check our model in a variety of situations it has to be applied to different experimental paradigms, e.g. polyrhythms of different order $N^r : N^l$.

V. SUMMARY

The analysis of physiological and psychological time series [12] is typically obstructed by intrinsic fluctuations and measurement noise. An additional problem is that our time series are rather short (12 cycles). Even for longer experimental observations, instationarities typically limit the length of data series which can be used for the analysis. Despite these difficulties we have shown that a coarse-graining of the data by transformation to symbol sequences can be successfully used to extract significant properties of the underlying dynamics.

In particular, our symbolic coding is well-adapted for the detection of qualitative changes in the behavioral dynamics. A qualitative transition from correct to incorrect timing of the rhythmic structure is transformed into a disorder–order transition in the symbol sequences [6,21]. This is quantitatively described by the Shannon entropy of the distribution of words, as a measure for stochasticity of the symbol sequences.

The existence of qualitative transitions in our experiment is an important finding for the modeling of simple movement tasks which are typically described by statistical timer–motor models [14]. These models are linear. Therefore, it is impossible to reproduce qualitative changes which we have proven to exist in the experimental data. The value of the timer–motor approach is to highlight the stochastic component in movement timing. This emphasizes the advantage of our model which combines the stochastic description of the timer–motor approach with a nonlinear control mechanism to account for both stochasticity and dynamical transitions.

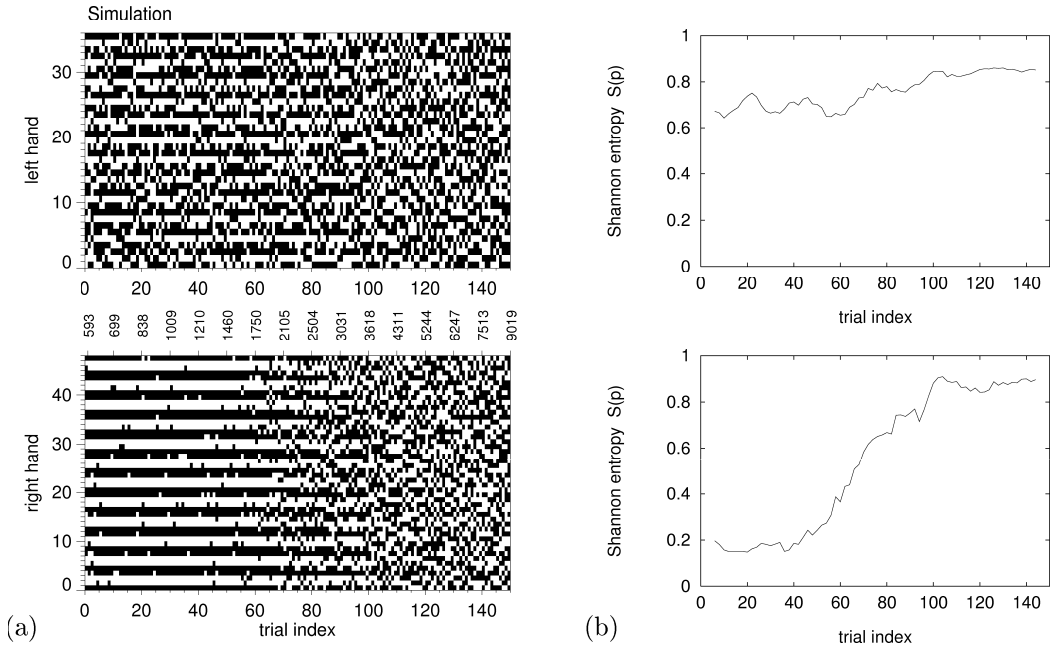

FIG. 8. Simulation of the model for bimanual production of polyrhythms using a linear variation of k_1^r. (a) The symbol patterns are in good agreement with those produced by subject B. On the basis of the Shannon entropy (b) it can be seen that the transition in the experimental data is rather sharp when compared to the simulation. This is a consequence of the strictly linear variation of the control parameter which may not apply for the experimental case.

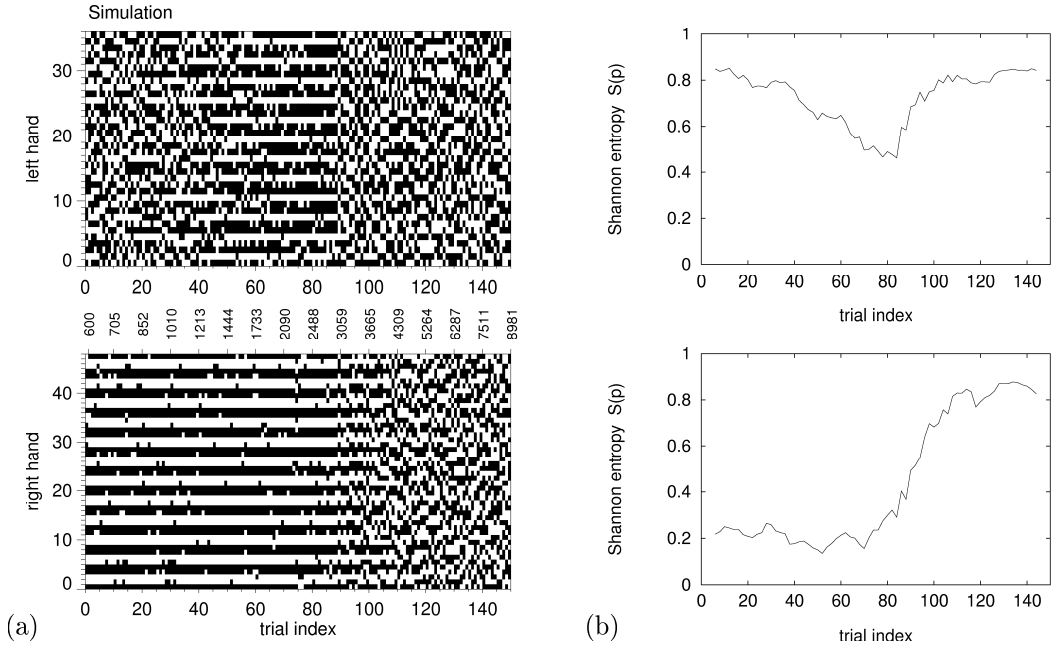

FIG. 9. Example for a simulation of the model in a more complicated case. The symbol patterns (a) and Shannon entropies (b) are qualitatively in agreement with those produced by subject A.

We have shown that our model reproduces the experimentally observed symbol patterns, if the discrete time delay is fixed at $d = 1$. The existence of such a time delay [23] is supported by physiological experiments [22], which show the ubiquity of delay processes. As an example, voluntary movements are initiated by firing of motor neurons with a time delay of order 100 ms. If these movements are disturbed by some external influence, then an additional increase of activity in the motor cortex is observed after 20 ms. A reasonable estimate of a time delay between brain processes and observed movements will be bounded within these limits. Since the shortest intervals of the polyrhythm task are about 50 ms, we expect time delayed error correction, $d = 1$, in the theoretical model.

Additional support for the concept of time–delayed error correction arises from an experimental study, where subjects were required to synchronize their movements with a metronome. In the analysis based on the concept of two–level timing, time–delayed error correction has been found for fast tempi [25]. This corresponds to $d = 1$ for the error correction in our model.

Recently the impact of artificial delays on visually guided movements was used to analyze the feedback loop in detail [24]. The importance of time delay in feedback loops, which is emphasized by our results, suggests that artificial delays of (auditory) feedback might be a promising approach for the experimental study of the production of rhythms.

In this work we have shown that the stochastic properties of timing structures interact with the nonlinear dynamics. Therefore, dynamical models [1] and statistical two–level models [14] were combined to understand the variability of movement control. In this sense, our approach may be able to bridge the gap between two methodological and theoretical traditions in the more general discussion about stochastic versus deterministic aspects of simple movement tasks.

ACKNOWLEDGMENTS

It is a pleasure to acknowledge many conversations on modeling with A. Zaikin and on data analysis with U. Schwarz who shared with us the work on the analysis of polyrhythms. We thank D. Vorberg, who drew our attention to the stochastic processes in the analysis of movements, and P. Tass for comments on the manuscript. This research is part of the interdisciplinary project Formal Models of Cognitive Complexity at the University of Potsdam. The project is funded by the grant INK 12/A1 (project B1) of the German Research Foundation (DFG).

[1] H. Haken, *Principles of Brain Functioning* (Springer, Berlin – Heidelberg – New York, 1996); J.A.S. Kelso, *Dynamic patterns. The self-organization of brain and behavior* (MIT Press, Cambridge/MA, 1995).

[2] H. Haken, J.A.S. Kelso and H. Bunz, Biol. Cybern. **51**, 347 (1985).

[3] M. Wiesendanger, O. Kazennikov, S. Perrig and P. Kaluzny, in: *Hand and Brain, The Neurophysiology and Psychology of Hand Movements*, edited by A.M. Wing, P. Haggard and J.R. Flanagan (Academic Press, London, 1996).

[4] J.A.S. Kelso, D.L. Southard and D. Goodman, J. Exp. Psychol.: Human Percept. Perform. **5**, 229 (1979); S. Swinnen, H. Heuer, J. Massion and P. Casaer (eds.), *Interlimb coordination: Neural, dynamic, and cognitive constraints* (Academic Press, San Diego/CA, 1994).

[5] R.T. Krampe, R. Kliegl, U. Mayr and R. Engbert, (1996, submitted).

[6] R. Engbert, C. Scheffczyk, R.T. Krampe, J. Kurths and R. Kliegl, in [12].

[7] J.A.S. Kelso and G.C. deGuzman, in *Neural and Synergetic Computers*, edited by H. Haken (Springer, Berlin, 1988).

[8] P.J. Treffner and M.T. Turvey, J. Exp. Psychol.: Human Percept. Perform. **19**, 1221 (1993).

[9] C.E. Peper, P.J. Beek and P.C. van Wieringen, Biol. Cybern. **73**, 301 (1995).

[10] H. Haken, C.E. Peper, P.J. Beek and A. Daffertshofer, Physica D **90**, 179 (1996).

[11] CHAOS (Focus issue: *Dynamical disease: Mathematical analysis of human illness*) **5**, 1-209 (1995).

[12] H. Kantz, J. Kurths and G. Mayer-Kress (eds.), *Nonlinear analysis of physiological data* (Springer, Berlin – Heidelberg – New York, 1997, in press).

[13] J.J. Summers, D.A. Rosenbaum, B.D. Burns and S.K. Ford, J. Exp. Psychol.: Human Percept. Perform. **19**, 416 (1993).

[14] D. Vorberg and A.M. Wing, in *Handbook of perception and action, Vol. 3*, edited by H. Heuer and S.W. Keele (Academic Press, London, 1996).

[15] B.-L. Hao, Physica D **51**, 161 (1991); and refs. therein.

[16] R. Wackerbauer, A. Witt, H. Atmanspacher, J. Kurths and H. Scheingraber, Chaos, Solitons & Fractals **4**, 133 (1994); and refs. therein.

[17] P.I. Saparin, M.A. Zaks, J. Kurths, A. Voss and V.S. Anishchenko, Phys. Rev. E **54**, 737 (1996); J. Kurths, A. Voss, P. Saparin, A. Witt, H.J. Kleiner, N. Wessel, in [11].

[18] J. Guckenheimer and P. Holmes, *Nonlinear Oscillations, Dynamical Systems, and Bifurcations of Vector Fields* (Springer, New York – Berlin – Heidelberg, 1983).

[19] C. Scheffczyk, A. Zaikin, M. Rosenblum, R. Engbert, R. Krampe and J. Kurths, Intern. J. Bif. Chaos (1997, in press).

[20] R. Ivry, S.W. Keele, and H.C. Diener, Exp. Brain Res. **73**, 167 (1988).

[21] M. Schiek, F.R. Drepper, R. Engbert, H.-H. Abel and K. Suder, in [12].

[22] R.F. Schmidt and G. Thews, *Human Physiology* (Springer, Berlin – Heidelberg – New York, 1989).

[23] M.C. Mackey and L. Glass, Science **197**, 287 (1977); M.C. Mackey and J.G. Milton, Ann. N.Y. Acad. Sci. **504**, 16 (1988).

[24] P. Tass, J. Kurths, M.G. Rosenblum, G. Guasti and H. Hefter, Phys. Rev. E **54**, 2224 (1996); P. Tass, A. Wunderlin and M. Schanz, J. Biol. Phys. **21**, 83 (1995).

[25] D. Vorberg and H.-H. Schulze, (in preparation).